Excitonic exchange splitting and Stokes shift in Si nanocrystals and Si clusters

Toshihide Takagahara
NTT Basic Research Laboratories, 3-1, Morinosato Wakamiya, Atsugi, Kanagawa 243-01, Japan

Kyozaburo Takeda
Department of Materials Science and Engineering, School of Science and Engineering, Waseda University, 3-4-1, Ohkubo, Shinjuku, Tokyo 169, Japan

(Received 27 November 1995)

The size dependence of the electron-hole exchange interaction in Si nanocrystals is investigated and the excitonic exchange splitting is predicted to be as large as 300 meV in extremely small Si clusters. The exciton-phonon interaction in Si nanocrystals for acoustic phonon modes is formulated to calculate the Stokes shift and the Huang-Rhys factor. It is found that the observed onset energy of photoluminescence can be interpreted mainly in terms of the excitonic exchange splitting, although the contribution from the Stokes shift is not negligible. The importance of the self-consistent determination of the effective dielectric constant of Si clusters including the excitonic effect is demonstrated in view of the possibility of resolving the large discrepancy between theories and experiments concerning the size dependence of the exciton energy.

In the last few years, the visible photoluminescence from porous Si has attracted much attention from the fundamental physics viewpoint and from the interest of potential application to optical devices.[1,2] However, the mechanism of the photoluminescence is still controversial. In order to resolve the controversy, it is necessary to study finely the excitonic energy spectra in Si nanocrystals by size-selective spectroscopies[3,4] and to compare them with theoretical calculations. Recently, from the onset energy of photoluminescence and from the temperature dependence of the luminescence lifetime, the singlet-triplet exchange splitting of the excitonic states was claimed to be measured as a function of the luminescence energy.[3] The observed splitting is of the order of 10 meV and is much larger than the bulk value.[5] This suggests strong enhancement of the electron-hole exchange interaction in a Si nanocrystal. On the other hand, Martin *et al.*[6] reported that the onset energy of photoluminescence cannot be explained in terms of the exchange splitting but may be partially ascribed to the Stokes shift due to acoustic-phonon modes. However, they dealt with the dielectric screening erroneously in the exchange integral and introduced some phenomenological assumptions about the exchange integrals and the phonon modes in nanocrystals whose validity is not quite obvious. On the other hand, in Ref. 3, the expression of the excitonic exchange splitting for the direct-gap material was used for Si nanocrystals. However, the justification of this simple-minded extension to the case of indirect-gap materials with a multiple-valley structure is not obvious.

In order to clarify these features and to search for a quantitative interpretation of the observed onset energy, we calculate the Coulomb and exchange integrals exactly and formulate the exciton-phonon interaction taking into account all the relevant acoustic-phonon modes. We calculate the excitonic energy spectra by the configuration-interaction method and find that the gross features of the observed onset energy can be reproduced well by the excitonic exchange splitting in contrast to the conclusion of Ref. 6, although some quantitative discrepancy remains. The agreement between the theory and the experiment becomes improved by including the contribution from the luminescence Stokes shift. Furthermore, we confirm the enhancement of the excitonic exchange splitting in extremely small Si clusters and demonstrate the importance of the self-consistent determination of the dielectric constant of Si clusters including the excitonic effect.

We calculate the subband states in nanocrystals employing the multiband effective-mass approximation[7] in which the eigenstate is represented by the Bloch function multiplied by an envelope function. We consider a spherical quantum dot embedded in an infinitely high barrier material in order to simplify the analysis but to retain the essential physics. The valence subband states are calculated based on the full Luttinger Hamiltonian[8–10] including the spin-orbit split-off bands and can be specified by L_j where L is the orbital angular momentum of the envelope function and j denotes the total angular momentum of the Bloch function. Concerning the electron subband states, the mass anisotropy in the six equivalent conduction band valleys is taken into account. The excitonic states are constructed by the configuration-interaction method from a linear combination of interband excitations. It is important to notice that the dielectric constant ϵ should not be included in the expression of the exchange integral. In the Bethe-Salpeter equation for the excitonic state, the Coulomb term can contain electron-hole bubble diagrams corresponding to the dielectric screening, whereas the exchange term cannot include such diagrams because they are improper diagrams.[11–13] Furthermore, it can be shown that in the small size regime the electron-hole exchange interaction is mainly determined by the short-range exchange interaction and is inversely proportional to R^3, where R is the radius of a nanocrystal.[14]

The dielectric constant to be used in the Coulomb integral is the static dielectric constant. This constant of a nanocrystal is smaller than that of the bulk material because of the dis-

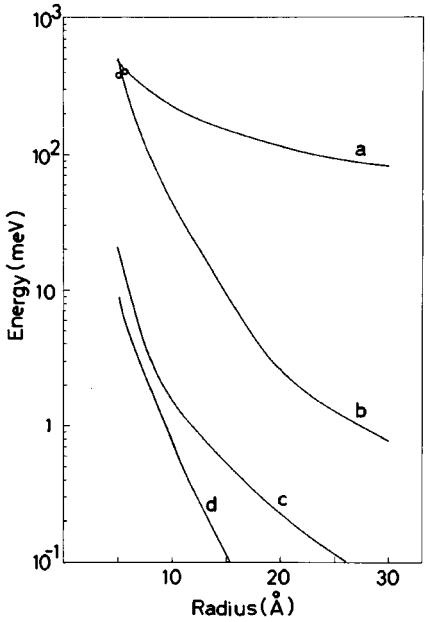

FIG. 1. The magnitude of the exchange and Coulomb energies are shown as a function of the radius of Si nanocrystals. The curve a (b) represents the intravalley Coulomb (exchange) energy $V_{\rm cl}(k_\Delta^\alpha, p_\alpha; k_\Delta^\alpha, p_\alpha)$ $[V_{\rm ex}(k_\Delta^\alpha, p_\alpha; k_\Delta^\alpha, p_\alpha)]$, where k_Δ^α and p_α denote the lowest electron subband state at the valley k_Δ^α and the highest valence subband state associated with a p_α-like Bloch function at the Γ point, respectively, and α is one of the Cartesian components. The curve c (d) shows the intervalley exchange (Coulomb) energy $V_{\rm ex}(k_\Delta^\alpha, p_\alpha; -k_\Delta^\alpha, p_\alpha)$ $[V_{\rm cl}(k_\Delta^\gamma, p_\alpha; -k_\Delta^\gamma, p_\beta)]$ where (α,β,γ) is a cyclic permutation of (x,y,z). The HOMO-LUMO exchange energies $E_{\rm ex}^{\rm HOMO\text{-}LUMO}$ for Si_8H_8 and $Si_{10}H_{16}$ molecules are plotted by circles.

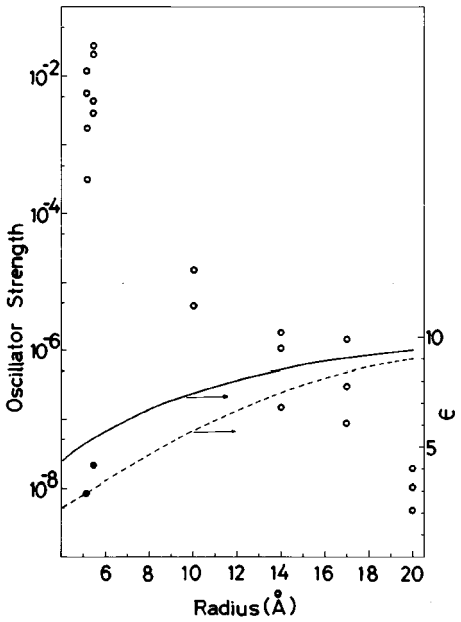

FIG. 2. The oscillator strengths of several prominent excitonic transitions are plotted by open circles for the $S_{3/2}$ multiplet for several values of the nanocrystal radius. The results for Si_8H_8 and $Si_{10}H_{16}$ molecules are shown at the effective radii in Table I. The self-consistently calculated dielectric constants for Si_8H_8 and $Si_{10}H_{16}$ molecules are exhibited by solid dots along with the results of the first-principles calculation (solid line) and of the generalized Penn's model (dashed line) in Ref. 6.

crete energy-level structure. According to a recent calculation without the excitonic effect,[15] the dielectric constant varies from ~ 8 to ~ 10 for radii from ~ 10 Å to ~ 20 Å. In the following calculation on nanocrystals, the size-dependent dielectric constant in the parametrized form is employed.

Owing to the symmetry of the Bloch functions and the envelope functions, the exchange and Coulomb integrals to be evaluated can be reduced to three kinds of integrals, namely, an intravalley integral and two types of intervalley integrals. The first type of the intervalley integral corresponds to a combination of two valleys at $k_\Delta^z = (0,0,k_\Delta)$ and $-k_\Delta^z = (0,0,-k_\Delta)$ and to its equivalent combinations, and the second type to a combination of two valleys at $k_\Delta^z = (0,0,k_\Delta)$ and $k_\Delta^x = (k_\Delta,0,0)$ and to its equivalents, where k_Δ denotes the magnitude of wave vector at the valley bottom. In Fig. 1, typical intravalley and intervalley Coulomb and exchange integrals are plotted as a function of the nanocrystal radius R. The strong enhancement of the intravalley exchange integral is seen and the typical R^{-3} dependence can be confirmed in the small size regime. The intravalley Coulomb integral exhibits a weaker size dependence that can be approximated by R^{-1}. The intervalley integrals are much smaller than the intravalley integrals and show strong size dependence similar to that of the intravalley exchange integral.

The valence subbands are split into $S_{3/2}$ and $S_{1/2}$ multiplets due to the spin-orbit interaction. The single electron-hole pair states composed of the $S_{3/2}$ $(S_{1/2})$ valence subband are 48 (24) -fold degenerate. The electron-hole exchange and Coulomb interactions intermix and split these degenerate states. The overall features of the excitonic spectra are dependent on the relative magnitude between the spin-orbit splitting energy and the exchange energy. In the case of radii >15 Å, the exchange energy is smaller than the spin-orbit splitting energy and thus the two multiplets are well-separated. On the other hand, in the case of radii <10 Å, the exchange energy is larger than the spin-orbit splitting energy and the mixing between the $S_{3/2}$ and $S_{1/2}$ multiplets becomes significant.

Another important feature is the oscillator strength of these excitonic transitions. The oscillator strengths of several prominent excitonic transitions of the $S_{3/2}$ multiplet are plotted in Fig. 2 by open circles for several values of the nanocrystal radius. For a nanocrystal with, e.g., 10 Å radius, the shortest radiative lifetime is ~ 200 μs as in the results of Ref. 6 and is about two orders of magnitude longer than the typical experimental observations. On the other hand, the lowest excitonic states in the $S_{3/2}$ multiplet are mostly composed of the spin-triplet component and are almost optically inactive. This is due to the high symmetry of the spherical shape. In actual nonspherical nanocrystals, as simulated by undulating ellipsoids in Ref. 6, the orbital degeneracy is lifted and the spin-singlet component is mixed into the lowest excitonic states, resulting in a finite radiative lifetime. Thus, although the two-level model proposed in Ref. 3 does not hold in a strict sense in a spherical nanocrystal, we can estimate the right order of magnitude of the excitonic exchange splitting employing the spherical nanocrystal model. The exchange splitting estimated from the energy-level splitting within the $S_{3/2}$ multiplet is plotted in Fig. 3 by a dashed line. The excitonic transition energies on the lower abscissa correspond to radii from ~ 14 Å to ~ 20 Å. We see that the

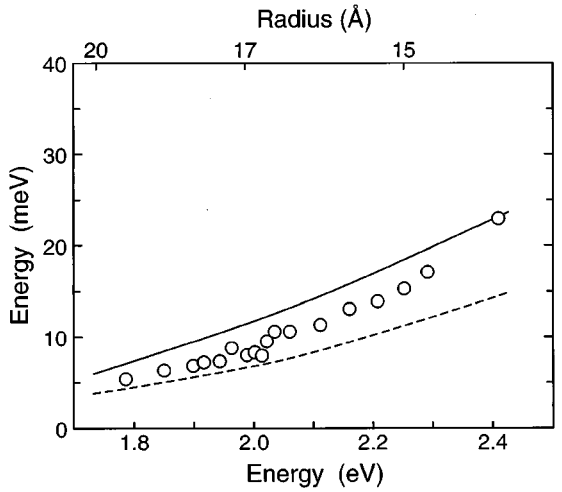

FIG. 3. The theoretical excitonic exchange splitting and the result including the Stokes shift are plotted by a dashed line and a solid line, respectively, as a function of the excitonic transition energy. The experimental data of Ref. 3 are exhibited by circles. On the upper abscissa, the nanocrystal radius is shown corresponding to the exciton energy in the lower abscissa.

gross features of the experimental data are reproduced well, although some quantitative discrepancy remains.

Now we investigate the Stokes shift due to acoustic-phonon modes as another mechanism which yields the onset energy of photoluminescence. In nanocrystals, even the acoustic-phonon modes become discrete and their energies are proportional to the inverse of the nanocrystal size. Under the stress-free boundary condition for a spherical nanocrystal, there appear two kinds of eigenmodes, namely, torsional modes and spheroidal modes.[16] From the explicit form of the electron-phonon interaction in bulk Si,[17] we can derive the relevant Hamiltonian as in Ref. 18. Then the Stokes shift Δ and the effective Huang-Rhys factor S for the excitonic state in the Franck-Condon approximation are given as[19]

$$\Delta = 2\sum_j \gamma_j^2/\hbar\omega_j \quad \text{and} \quad S = \sum_j \gamma_j^2/(\hbar\omega_j)^2, \tag{1}$$

where γ_j is the coupling strength, $\hbar\omega_j$ is the phonon energy, and the summation is taken over relevant phonon modes denoted by j. Through a similar analysis to that in Ref. 18, we see that $\Delta(S)$ is inversely proportional to R^3 (R^2) in the small size regime. The maximum value of the Huang-Rhys factor S is found to be 0.3–0.7 for the nanocrystal radius from 20 Å to 14 Å, indicating the weak-coupling regime of the exciton-phonon interaction. However, the luminescence Stokes shift is not negligible and is of the order of several meV in the above size range. The Stokes shift is dependent on the excitonic levels. In the estimation of the onset energy of photoluminescence, the photon-absorbing state is identified with the excitonic state in the $S_{3/2}$ manifold having the largest oscillator strength, while the luminescent state is identified with that having the lowest energy when the Stokes shift is included. The onset energies estimated in this way are plotted in Fig. 3 by a solid line. The quantitative agreement between the experiment and the theory is improved and can be regarded as satisfactory. An important conclusion here is that the observed onset energy of photoluminescence can be explained mainly in terms of the excitonic exchange splitting in contrast to the conclusion of Ref. 6, although the contribution from the Stokes shift is not negligible.

According to Fig. 1, the exchange energy seems to dominate over the Coulomb energy for the radius < 5 Å, suggesting a possible instability of the singlet exciton. However, in this size regime, more careful analysis is necessary. Hence, as examples of extremely small Si nanocrystals, we consider Si clusters having the cubane (Si_8H_8) and adamantane ($Si_{10}H_{16}$) structures and investigate the consistency with the asymptotic limit of the effective-mass theory concerning the excitonic exchange splitting, the dielectric constant, and the exciton oscillator strength. The electronic structures of these clusters are calculated by the first-principles local-density-functional method using Gaussian-type orbitals.[20] The bond lengths are chosen as 2.35 Å for the Si-Si bond and 1.54 Å for the Si-H bond, respectively, without optimization of the molecular structure. In both molecules, the HOMO (highest occupied molecular orbital) and LUMO (lowest unoccupied molecular orbital) levels are triply degenerate. It is worth noticing that the HOMO-LUMO gap energy (3.57 eV) of the Si_8H_8 molecule is smaller than that (5.67 eV) of the $Si_{10}H_{16}$ molecule contrary to the expectation based on the quantum confinement effect. This is due to the difference in the molecular structure. The $Si_{10}H_{16}$ molecule has a diamondlike skeleton structure and the electronic structure around the HOMO-LUMO gap is determined by the $p\sigma$ bonding orbitals. On the other hand, the Si_8H_8 molecule has a cubic structure that is incompatible with the sp^3 bonding and the $p\pi^*$ antibonding states are mixed into the occupied molecular orbitals, pushing up the HOMO levels. As a consequence, the HOMO-LUMO gap energy of the Si_8H_8 molecule is smaller than that of the $Si_{10}H_{16}$ molecule.

The excitonic states can be constructed from a linear combination of single-particle excitations across the HOMO-LUMO gap. In general, the dielectric constant is determined by the excitonic structure of the material system and, in turn, the excitonic structure is determined by the dielectric constant through the eigenvalue equation. Thus the dielectric constant and the excitonic structure have to be determined self-consistently. In the following we assume a local and uniform effective dielectric constant within a cluster in order to simplify the analysis but to see qualitative features. The static effective dielectric susceptibility of a cluster within the linear response theory can be expressed as

$$\chi_{\alpha\beta}(\omega=0) = \frac{1}{V}\sum_{\lambda}\left[\frac{\langle 0|P_\alpha|\lambda\rangle\langle\lambda|P_\beta|0\rangle}{E_\lambda - i\hbar\gamma_\lambda} + \frac{\langle 0|P_\beta|\lambda\rangle\langle\lambda|P_\alpha|0\rangle}{E_\lambda + i\hbar\gamma_\lambda}\right], \tag{2}$$

where the summation is taken over the excitonic states denoted by $|\lambda\rangle$ and $\hbar\omega_\lambda$ and γ_λ are the energy and the damping constant of the $|\lambda\rangle$ state, $|0\rangle$ the ground state of the cluster, P the total electronic polarization vector, and α and β denote the Cartesian components. In the actual calculation, γ_λ is neglected and the effective radius R_{eff} of a cluster is estimated from the spherical approximation of the charge distribution function of all valence electrons and V is identi-

TABLE I. Effective radius $R_{\rm eff}$, the dielectric constant ϵ (free) calculated without the excitonic effect, the self-consistently calculated dielectric constant ϵ(SCC), the exchange (Coulomb) energy $E_{\rm ex}^{\rm HOMO\text{-}LUMO}$ ($E_{\rm cl}^{\rm HOMO\text{-}LUMO}$) between HOMO and LUMO levels and the excitonic exchange splitting $\Delta_{\rm ex}$ are listed for Si_8H_8 and $Si_{10}H_{16}$ molecules.

	Si_8H_8	$Si_{10}H_{16}$
$R_{\rm eff}$ (Å)	5.15	5.48
ϵ(free)	4.01	6.99
ϵ(SCC)	2.89	4.17
$E_{\rm ex}^{\rm HOMO\text{-}LUMO}$ (meV)	390	402
$E_{\rm cl}^{\rm HOMO\text{-}LUMO}$ (eV)	1.92	0.96
$\Delta_{\rm ex}$ (meV)	298	225

fied with $4\pi R_{\rm eff}^3/3$. The excitonic states are calculated by the configuration-interaction method including 20 (28) occupied levels and 20 (28) unoccupied levels in the ascending order of energy for the Si_8H_8 ($Si_{10}H_{16}$) molecule.

Since the spin-orbit interaction is not included in this calculation, the spin-singlet and the spin-triplet excitonic states are completely separated and the exchange splitting can be unambiguously estimated. The obtained results are summarized in Table I. It is found that the maximum values of the exchange energy between HOMO and LUMO levels are of the order of 400 meV and are smaller than the Coulomb energy in contrast to a simple extrapolation of curves *a* and *b* to smaller sizes in Fig. 1, where the HOMO-LUMO exchange energies for Si_8H_8 and $Si_{10}H_{16}$ molecules are plotted by circles. The excitonic exchange splitting estimated for the two molecules is of the same order of magnitude as the HOMO-LUMO exchange energy because the lowest-energy excitons are preferentially composed of the HOMO-LUMO gap excitations. The maximum values of the Coulomb energy between HOMO and LUMO levels are as large as 1–2 eV. This fact suggests the importance of the reduced effective dielectric constant of Si nanocrystals in determining the size dependence of the exciton energy, about which a large discrepancy between theories and experiments was pointed out.[21] We notice the importance of the self-consistent calculation (SCC) including the excitonic effect from the comparison of ϵ(SCC) with ϵ(free), which is calculated without the excitonic effect. The results of ϵ(SCC) are plotted in Fig. 2 by solid dots and are found to be consistent with the results of the first-principles calculation and of the generalized Penn's model.[15]

In addition, the oscillator strengths of several lowest-energy excitonic transitions of Si_8H_8 and $Si_{10}H_{16}$ molecules are plotted in Fig. 2 by open circles. They seem to be aligned coherently with the results of the effective-mass theory for larger nanocrystals. Finally, in view of the R^{-3} dependence of the Stokes shift and the ~8-meV Stokes shift at $R=15$ Å, we expect the Stokes shift to be about 200 meV for Si_8H_8 and $Si_{10}H_{16}$ molecules, which is not inconsistent with the first-principles calculation of the Stokes shift for $Si_{29}H_{36}$.[22]

In conclusion, the size dependence of the electron-hole exchange interaction in Si nanocrystals is investigated and the excitonic exchange splitting in extremely small Si clusters is shown to be greatly enhanced. The exciton-phonon interaction in Si nanocrystals for acoustic-phonon modes is formulated to calculate the Huang-Rhys factor and the Stokes shift of photoluminescence. It is found that the observed onset energy of photoluminescence can be reproduced well by the excitonic exchange splitting, although the contribution from the Stokes shift is not negligible. The importance of the self-consistent determination of the effective dielectric constant of Si clusters including the excitonic effect is demonstrated in view of the possibility of resolving the large discrepancy between theories and experiments concerning the size dependence of the exciton energy. Furthermore, the coherency between the cluster calculation and the effective-mass theory is confirmed for the excitonic exchange integral and for the exciton oscillator strength.

One of the authors (T.T.) would like to thank Dr. L. E. Brus and Dr. M. S. Hybertsen for enlightening discussions in the early stage of this work.

[1] *Light Emission from Silicon*, edited by S. S. Iyer, R. T. Collins, and L. T. Canham, MRS Symposia Proceedings No. 256 (Materials Research Society, Pittsburgh, 1991).
[2] *Silicon-Based Optoelectronic Materials*, edited by M. A. Tischler, R. T. Collins, M. L. W. Thewalt, and G. Abstreiter, MRS Symposia Proceedings No. 298 (Materials Research Society, Pittsburgh, 1993).
[3] P. D. J. Calcott, K. J. Nash, L. T. Canham, M. J. Kane, and D. Brumhead, J. Phys. Condens. Matter **5**, L91 (1993).
[4] T. Suemoto, K. Tanaka, A. Nakajima, and T. Itakura, Phys. Rev. Lett. **70**, 3659 (1993).
[5] J. C. Merle, M. Capizzi, P. Fiorini, and A. Frova, Phys. Rev. B **17**, 4821 (1978).
[6] E. Martin, C. Delerue, G. Allan, and M. Lannoo, Phys. Rev. B **50**, 18 258 (1994).
[7] T. Takagahara and K. Takeda, Phys. Rev. B **46**, 15 578 (1992).
[8] J. M. Luttinger, Phys. Rev. **102**, 1030 (1956).
[9] A. Baldereschi and N. O. Lipari, Phys. Rev. B **8**, 2697 (1973).
[10] N. O. Lipari and A. Baldereschi, Solid State Commun. **25**, 665 (1978).
[11] Y. Abe, Y. Osaka, and A. Morita, J. Phys. Soc. Jpn. **17**, 1576 (1962).
[12] L. J. Sham and T. M. Rice, Phys. Rev. **144**, 708 (1966).
[13] A. Haug and W. Ekardt, Solid State Commun. **17**, 267 (1975).
[14] T. Takagahara, Phys. Rev. B **47**, 4569 (1993).
[15] L. W. Wang and A. Zunger, Phys. Rev. Lett. **73**, 1039 (1994).
[16] A. E. H. Love, *A Treatise on the Mathematical Theory of Elasticity* (Dover, New York, 1944).
[17] L. D. Laude, F. H. Pollak, and M. Cardona, Phys. Rev. B **3**, 2623 (1971).
[18] T. Takagahara, Phys. Rev. Lett. **71**, 3577 (1993).
[19] S in (1) is a sum of the Huang-Rhys factors for relevant phonon modes and represents the dimensionless coupling strength.
[20] K. Takeda and K. Shiraishi, Phys. Rev. B **39**, 11 028 (1989).
[21] S. Schuppler *et al.* Phys. Rev. Lett. **72**, 2648 (1994).
[22] M. Hirao and T. Uda, Int. J. Quantum Chem. **52**, 1113 (1994).